

A COMPARATIVE STUDY OF DISSIPATION RATES IN URBAN AND SUBURBAN ENVIRONMENTS USING SODAR DATA

Richard L. Coulter, Mikhail S. Pekour, and Timothy J. Martin
Argonne National Laboratory, Argonne, IL 60439, USA
William J. Shaw and J. Christopher Doran
Pacific Northwest National Laboratory, Richland, WA 99352, USA

Abstract

Data from field studies in Phoenix, AZ, during June 2001 and Oklahoma City, OK, during July 2003 are used to calculate the structure function of velocity by using the velocity differencing technique. We found that this technique can often be applied for these locations during summer, because strong solar forcing generates significant low-frequency energy in the turbulence spectrum. At other times, usually during stable nighttime conditions, this technique is inappropriate. During nighttime the method is sometimes useful at altitudes well above the surface — even when conditions near the surface are not sufficiently turbulent. This may be because the source of nighttime turbulence (the nocturnal low-level jet) is well above the surface, particularly in Oklahoma City. For a total of seven different sites in the two field studies, we compare velocity structure parameters, dissipation rates, and vertical velocity variances within the urban heat island (including measurements from the top of a building) and in suburban locations.

Keywords: sodar, turbulence, dissipation rate, velocity structure parameter, urban

1. Introduction

During the summers of 2001 and 2003, respectively, campaigns in Phoenix, AZ, and Oklahoma City, OK, measured, among other things, wind profiles and turbulence within the atmosphere's mixed layer. The 2001 Phoenix Sunrise field study (PHX01) on 13–30 June 2001 was designed to investigate the rapidly developing early morning mixed layer and its impact on atmospheric chemical transformation and transport (Doran et al., 2003); it used a combination of radar wind profiler-minisodar deployments, balloon-borne meteorological profiles, and chemical measurements (from aircraft, the ground, and buildings) throughout the Phoenix area. The Joint Urban 2003 (JU03) field study (27 June–31 July 2003) in Oklahoma City investigated urban dispersion by using a wide variety of turbulence instrumentation, tracers, and monitoring equipment during ten intensive operating periods (IOPs), in addition to wind and

temperature profiling instrumentation (radar wind profiler-minisodar combinations and balloon-borne meteorological parameter profilers), in both daytime and nighttime. In this paper we explore the use of minisodar (Coulter and Martin, 1986) data to estimate and compare turbulence dissipation rates from disparate urban and suburban locations.

Estimates of the temperature and velocity structure functions, C_T^2 and C_V^2 , respectively, have often been the goal of sodar investigations. Estimates of C_T^2 are especially common. Estimating C_V^2 with sodar data is generally approached in one of two ways: (1) from the amplitude of the scattered acoustic signal in multiple directions, with the relation (e.g., Clifford, 1972)

$$\sigma(\theta) = \frac{\cos^2(\theta) \left[\frac{C_v^2}{c^2} \cos^2\left(\frac{\theta}{2}\right) + 0.13 \frac{C_T^2}{T^2} \right]}{18.2 l^{1/3} \sin^{1/3}\left(\frac{\theta}{2}\right)}, \quad (1)$$

where σ is the scattering cross section at angle θ , l is the acoustic wavelength, c is the speed of sound, and T is the atmospheric temperature; or (2) from the definition of C_v^2 ,

$$C_v^2 = \frac{\overline{[u(x) - u(x+l)]^2}}{l^2}, \quad (2)$$

where l is the separation between two simultaneous measurements of a component of the wind speed, one of which is at location x , and the overbar indicates an ensemble average. The first method has been used successfully (e.g., Thomson et al., 1978), though it is complicated by the difficulty of defining intersection volumes of transmitted and received acoustic energy at scattering angles other than 180 deg and the necessity for accurate calibration of acoustic sources and receivers.

The second method is more easily implemented (see, e.g., Veill et al., 1988; Coulter, 1990); however, it also has limitations, including (1) values of $u(x)$ and $u(x+l)$ that are not precisely simultaneous; (2) an inherent volume average in the individual estimates of u that effectively removes some extreme values, leading to an underestimate of D ; and (3) reliance of eq. (2) on the assumption that l is within the inertial subrange of turbulence (and that a Kolmogorov spectrum of turbulence prevails). The last of these limitations is perhaps the most serious, because the separation distances imposed by conventional sodars is large enough to put its assumption in question. One important method of testing relies on the fact that C_v^2 should be constant; thus, the velocity structure parameter,

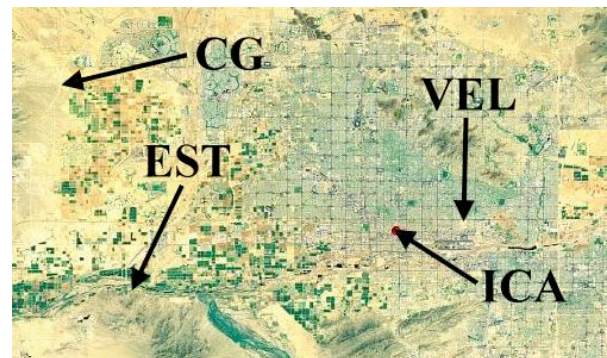
$$D = \overline{[u(x) - u(x+l)]^2}, \quad (3)$$

should increase linearly as ρ^3 increases. For use with sodar, l is usually defined either by the number of range gates between values of u , separated in time by a few milliseconds (the number of range gates divided by c), or by the time between measured values of u at a single range gate, in which case l is defined by the

product of the pulse period and the mean wind. The assumption of a linear increase of D with ρ^3 (constant C_v^2) is strictly true only when l is in the horizontal direction, whereas in the convective boundary layer, C_v^2 generally changes with height (Asimakopoulos et al., 1983). On the other hand, when a single range gate is used, the time separation between pulses (1–4 s) forces larger values of l than are encountered with l along the pointing direction of the sodar antenna.

2. Instrument Deployment

During the PHX01 study we placed four minisodars at locations in downtown Phoenix (at VEL and ICA; Fig. 1) and in suburban to rural surroundings (EST and CG; Fig. 1). The Vehicle Emissions Laboratory (VEL) site was on the eastern edge of the business district; a freeway approximately 0.5 km away bounds an open industrial area to the north. At the Industrial Commission of Arizona (ICA) site, a small antenna (one-half the size of the other antennae and unprotected from precipitation) was mounted on the roof of a building, 30 m above the ground. The Estrella (EST) site was in an unoccupied trailer park next to a golf course, and the Citrus Grove (CG) site in Waddell, was within a citrus grove surrounded by open, very sparsely vegetated land, operated by Arizona State University, with desert immediately to the west (see Fig. 1).



One of our goals in JU03 was to study the Figure 1. Minisodar measurement locations in the Phoenix area. The horizontal span covers approximately 57 km.

During this field study, conditions in Phoenix were extremely hot and dry, with daytime temperatures regularly above 40°C and the height of the mixed layer (z) often exceeding 3 km during the afternoon. Almost no precipitation fell during this

period. (Normally, a monsoon season begins in mid to late July.) Winds were generally light, but blowing sand and sometimes lightning accompanied occasional strong, highly localized nighttime windstorms.

One of our goals in JU03 was to study the modification of the mixed layer by an urban region. Because the prevailing winds are generally southerly at Oklahoma City, we used four sites along a N-S line (Fig. 2). The Botanical Gardens (BG) site, at the intersection of Reno and Walker streets was in a small parking lot surrounded by relatively lush garden vegetation (approximately 200m x 200m) within the urban center. Because of the impacts of sodar noise on the public, the system was operated primarily during nighttime, except for daytime IOPs. The site at the intersection of 10th and Harvey streets (RH), operational only after 13 July, was on the northern edge of the urban center, with 10-20-m-high buildings on the east and west. The Goodholme Park (GP) site data were not used in this analysis. The First Christian Church (CC) site, just north of 36th street, was in a suburban location with a freeway (running north-south) about 0.3km to the east and relatively open, vegetated land in the surrounding 200-m x 200-m area, except for a low (10-m-high) building immediately to the south and a 20-m x 50-m parking lot immediately to the northwest.

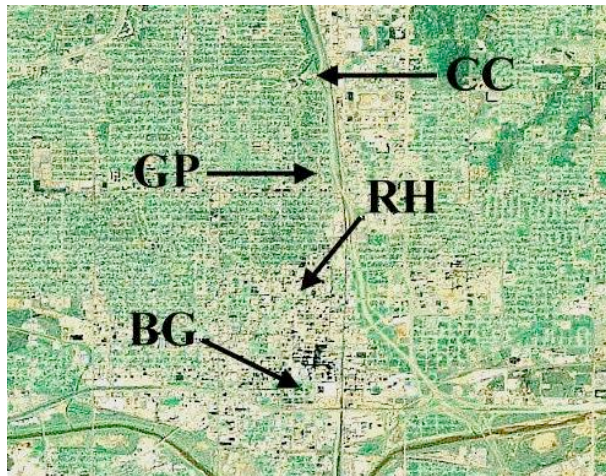


Figure 2. Argonne minisodar measurement locations in the Oklahoma City region. The north-south extent of the figure is approximately 10km.

Weather conditions during the period were milder but more variable than during PHX01, with daytime maximum temperatures near 35°C and

occasional rainfall. The daytime mixed layer was generally less than 3km and occasionally less than 2km. In addition to effects of the urban heat island, nighttime occurrences of the low-level jet were common, with wind speed maxima near 20m s⁻¹ within the lowest 250m.

3. Data Analysis

To test the applicability of eq. (2) to the data from all the locations, we made calculations of D by using the vertical component of motion, w , varying l from 1 range gate (5m) to 17 (85m) at base heights between 20 and 80m. Corrections for volume averaging and overlapping volumes for neighboring range gates were applied according to the approach of Kristensen (1978). Additional calculations made by using sequences of w at a single range gate and l determined by the horizontal wind speed are not discussed here in detail, but horizontal and vertical approaches agreed fairly well at comparable separations. An averaging time of 25 min was used at sites that included RASS temperature measurements (CG, EST, VEL, CC); otherwise 30 min was employed. Figures 3 and 4 illustrate the diurnal variation of D during PHX01 at the CG site and JU03 at the CC site, respectively. (Results for other sites and times are similar in form, if not in detail.)

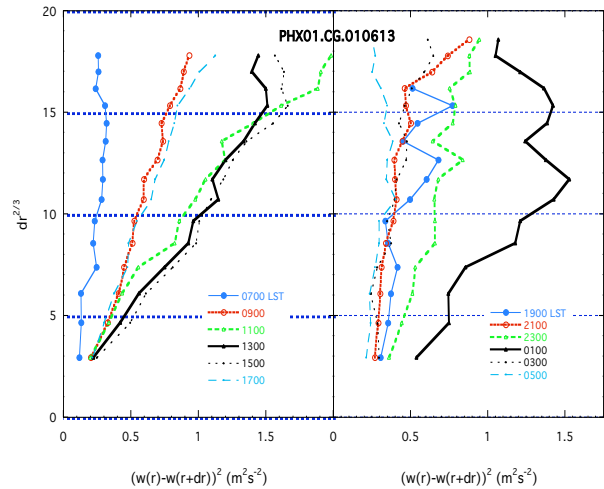


Figure 3. Variation of D with increasing l during daytime (left) and nighttime (right) during PHX01 at the CG site (location in Fig. 2).

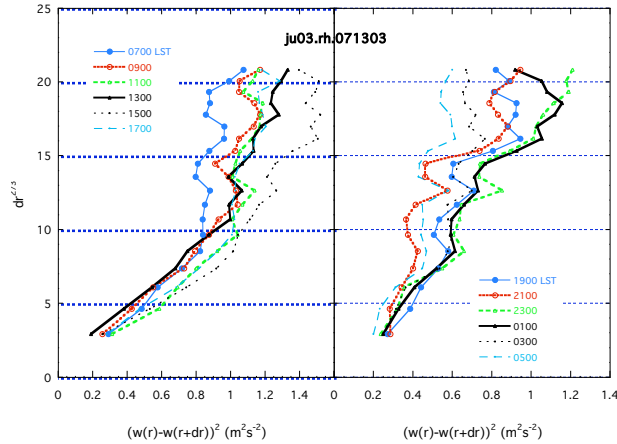


Figure 4. Variation of D with increasing l during daytime (left) and nighttime (right) during JU03 at the CC site (location in Fig. 2).

The linearity of the relationship between D and l is apparent during daytime at both sites. The distance over which the relationship is linear varies with time and appears to be somewhat larger during JU03. However, variation of C_v^2 with height can affect the perceived linearity of the profile, as we observed (see Section 3.1). The increasing slope with time during the day is consistent with strong solar heating at the surface and increasing turbulence energy. It is tempting to relate the maximum in the linear portion of the plots to the wave number of the expected peak in the energy spectrum (Kaimal, 1973). However, such a relationship is not likely with these results (obtained by using vertical separations), because the range of the minisodar is too limited for large separations. Nevertheless, the observed increase in the maximum separation with time is encouraging.

Even during nighttime, there is evidence of a linear relationship, albeit a more noisy one than during daytime, at small ranges. This is misleading; this interpretation is compromised by the nighttime non-zero x intercept ($l = 0$) value (extrapolated from the straight-line portion), in contrast to daytime intercepts. This observation suggests that the turbulence region of the velocity spectrum is shifted to higher frequencies during stable nocturnal conditions and that eq. (2) is inappropriate at these times and separations. At other times, however, eq. (2) may apparently be used during nighttime. Figure 5 illustrates this by comparing linearity plots of D with different base heights during JU03.

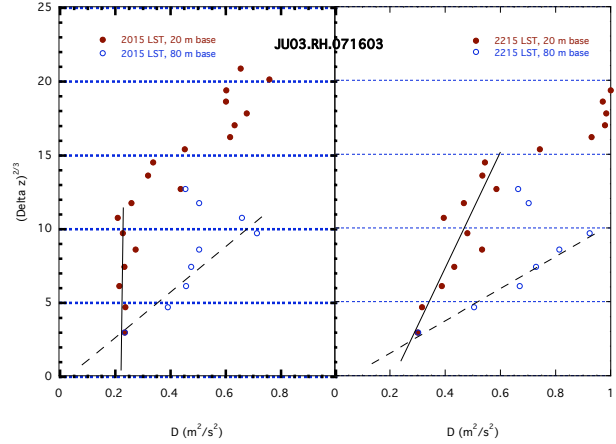


Figure 5. Variation of D with increasing l during night with 20-m (left) and 80-m (right) base heights for JU03 at the RH site.

The x intercept value is very nearly zero for base heights of 80 m, in contrast with simultaneous values at 20 m, perhaps because the source of the nocturnal turbulence is aloft in the midwestern United States (Mahrt and Vickers, 2002) as a result of the presence of the low-level wind maximum near 250 m.

3.1. Dissipation Rates

For a Kolmogorov spectrum of turbulence, the dissipation rate, ϵ can be calculated from

$$\epsilon = 0.36(C_v^2)^{3/2}. \quad (4)$$

Figure 6 shows the mean daytime variation of the profiles of C_v^2 during the two field studies, while Fig. 7 shows the mean daytime (0900–1700 LST) values of dissipation rate within the lowest 100 m from all IOPs. A separation of 15 m (3 range gates) was used (to reduce sample volume overlap) and correction factors have been applied for the overlap of sampling volumes for small l and the sampling volume size described by Kristensen (1978). In spite of day-to-day variability, the forms of the profiles were very consistent (data not shown). The presence of enhanced low-level turbulence at CC and RH relative to BG is a major feature of the data for JU03. Apparently the vegetation at BG reduced the overall turbulence levels within the lowest portions of the profile. At heights near 100 m, turbulence values at BG exceeded those at the other sites, as mechanical

turbulence created by slightly more distant buildings became important. The small values observed at ICA in PHX01 remain somewhat puzzling. The enhanced values near the surface (actually on the rooftop, 30 m above street level) for ICA are consistent with mechanical turbulence from flow over an elevator shaft approximately 8 m high. Above that, however, the values are significantly smaller than at the other sites.

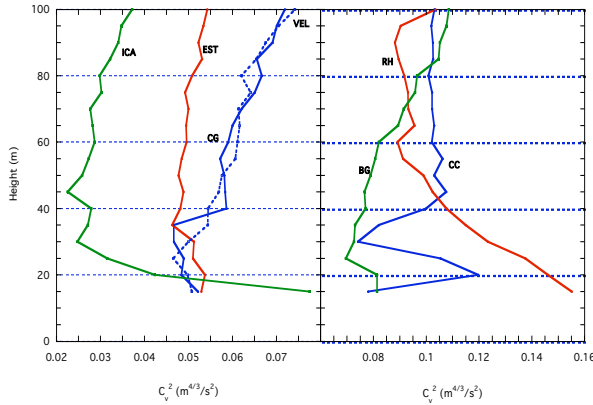


Figure 6. Mean daytime profiles of the velocity structure function during PHX01 (left) and JU03 (right). Note the larger abscissa scale on the right. Echoes and the wake of a small building (20 m) affected JU03 data at CC (at 20–40 m) during southerly wind conditions.

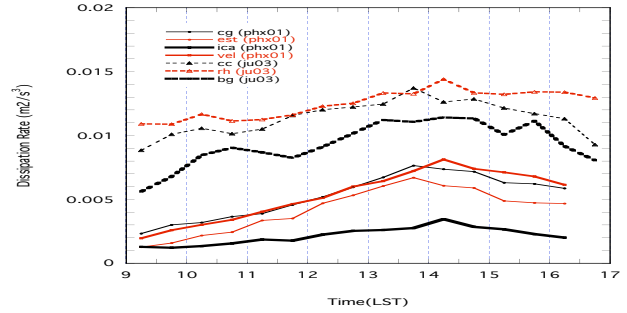


Figure 7. Daytime variation of dissipation rate, averaged through 100 m, at all sites in PHX01 and JU03.

Overall, the dissipation rates observed at Phoenix were roughly 33% of those observed in Oklahoma City. The most likely reason for this difference is that the median wind speeds between 15 and 100 m was larger during JU03 (4.8 m/s) than during PHX01 (3.4 m/s). However, scaling of the dissipation rates with s^3/z , where s is the wind speed and z is the measurement height does not account for the observed differences (Table 1, PHX01 values are 70% of JU03 values), although the dissipation rates are linearly correlated with s^3/z . If s^3/z_i is used as the scaling parameter, significantly more of the difference is accounted for (Table 1, PHX01 values are 42% of JU03 values). Even so, there remains an unexplained difference in the observed dissipation rates at the two sites.

Site	Phoenix Sunrise Experiment 2001					Joint Urban Experiment 2003			
	CG	EST	ICA	VEL	Mean	CC	RH	BG	Mean
$\overline{\epsilon}$ (m^2s^{-3})	0.0050	0.0040	0.0024	0.0052	0.0041	0.012	0.013	0.011	0.012
s^3/z (m^2s^{-3})	2.15	1.22	1.07	1.46	1.47	2.60	2.16	1.51	2.09
s^3/z_i (m^2s^{-3})	0.052	0.045	0.039	0.037	0.043	0.13	0.09	0.087	0.102

Table I. Values of dissipation rate and scaling parameters averaged over all measurement days and between 15 and 100 m above the surface (rooftop for ICA) at all sites.

3.2. Vertical Velocity Correlations

We can expand eq. (3) by using the vertical component of motion, w , to find

$$l^{2/3}C_v^2 = \overline{w^2(z) + w^2(z+l) - 2w(z)w(z+l)}, \quad (5)$$

which becomes

$$l^{2/3}C_v^2 = \overline{\sigma_w^2(x) + \sigma_w^2(x+l) - 2w(x)w(x+l)}, \quad (6)$$

where $\sigma_w^2(x)$ is the standard deviation of vertical velocity, and we assume that the mean vertical motion is negligible at both locations. Then

$$\frac{l^{2/3}C_v^2}{\overline{\sigma_w^2(x) + \sigma_w^2(x+l)}} = 1 - \frac{\overline{\sigma_w(x)\sigma_w(x+l)}}{\overline{\sigma_w^2(x) + \sigma_w^2(x+l)}} \text{Co}[w(x), w(x+l)]$$

where $Co[w(x), w(x + l)]$ is the correlation between the vertical motion at x and $x + l$. For a vertical separation of 15m (3 range gates), the coefficient of the correlation in the second term on the right side of

eq.(7) is nearly 1. Figures 8 and 9 show how this relationship varies with height during daytime at all sites in the studies on selected days (most days during PH01 and IOP days during JU03).

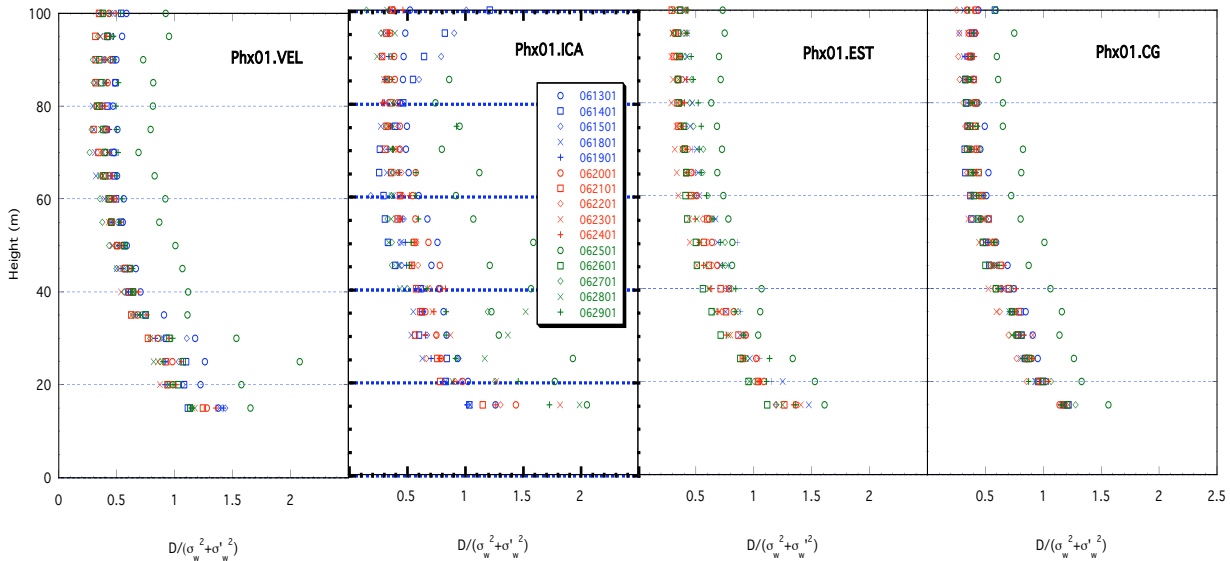


Figure 8. Daily averaged profiles of the ratio of the structure parameter to the standard deviation of vertical velocity during PHX01. The velocity samples are separated by 3 range gates or 15m , and the lower height is plotted. Even so, values were larger (with smaller correlation between vertically separated vertical velocities) at all sites and heights on 25 June (o).

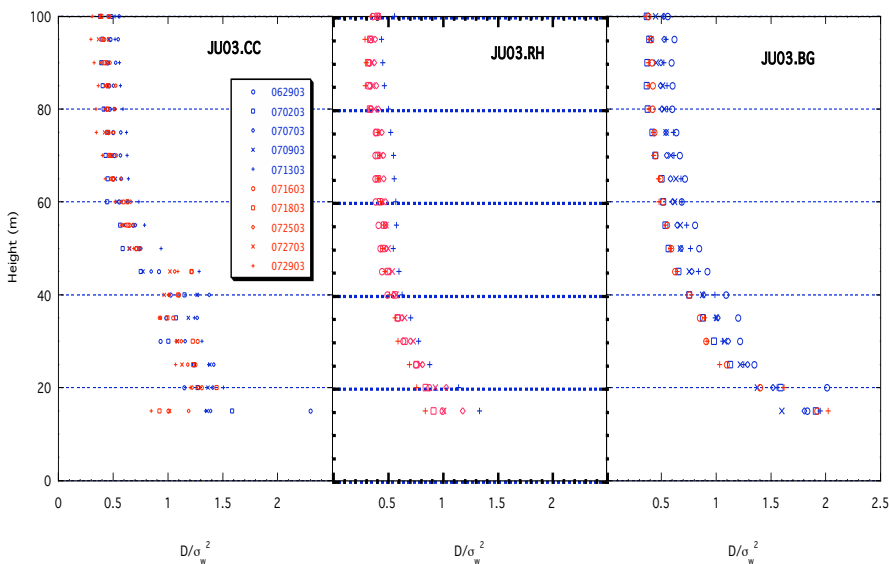


Figure 9. As for Fig. 8 during JU03. Echoes at the CC site adversely affected data at 25–50m. Note also that data collection at the RH site did not begin until 13 July, and thus fewer values are plotted.

A value of 1 in these plots indicates essentially no correlation between vertical motions separated by 15 m, and a value of 0 indicates perfect correlation.

The similarity of the profiles in Figs. 8 and 9 from day to day and from site to site is notable. There is generally little correlation near the surface, with values increasing steadily with height. This observation agrees with the concept that the vertical motion in the boundary layer is controlled principally by coherent, primarily vertically oriented thermal circulations that scale with height above the surface. Thus at heights near 20 m, the sensed values 15 m higher are likely uncorrelated or even negatively correlated because of their substantially different locations within the circulation. At heights near 100 m, on the other hand, a separation of 15 m corresponds to only a slight displacement within the dominant thermal plume structure.

Values of the ratio are significantly larger at all sites on June 25 2001 during PH01. On this day, average wind speeds during the afternoon approached 20 m/s during a frontal passage as winds shifted from SW to NW. Values at the BG site (JU03; Fig. 9) are noticeably larger near the surface than at any of the other sites (values > 1 below 35 m); this result may be associated with the heavily watered foliage in the immediate 200- to 200-m vicinity that includes the Botanical Gardens, which tends to discourage vigorous thermals near the surface, in addition to suppressing dissipation rates.

4. Conclusions

Unaveraged minisodar data collected during the PHX01 and the JU03 experiments were used to calculate dissipation rates and vertical velocity correlations at 15-m separations at heights of 20–100 m. Average daytime dissipation rates of approximately $0.004 \text{ m}^2 \text{ s}^{-3}$ prevailed in Phoenix, versus $0.01 \text{ m}^2 \text{ s}^{-3}$ in Oklahoma City. The difference is likely due to the larger wind speeds and deeper mixed layer in Phoenix. The smallest values were encountered at the top of a building in Phoenix ($0.002 \text{ m}^2 \text{ s}^{-3}$) and in the Botanical Gardens in central downtown Oklahoma City ($0.009 \text{ m}^2 \text{ s}^{-3}$). Although we generally could not use the velocity differencing technique to estimate structure functions during nighttime, this was occasionally possible at larger heights (80 m) in Oklahoma City, where the low-level

nocturnal jet apparently is a source of enough wind shear to generate turbulence.

Values of the ratio of the velocity structure parameter to the vertical velocity variance were found to be remarkably consistent from day to day and from site to site. Further investigation using horizontal spacing to estimate the structure parameter will shed light on the ability to estimate the peak of the energy spectrum with this technique. Incorporation of data from the GP site during the JU03 study should enable calculation of values from larger heights, because lower frequencies were used with that system.

5. Acknowledgements

This work was supported by the U.S. Department of Energy, Office of Science, Office of Biological and Environmental Research, under contract W-31-109-Eng-38, and by the Defense Threat Reduction Agency.

6. References

- Asimakopoulos, D.N., Mouldsley, T.J., Helmis, C.G., Lalas, D.P., and Gaynor, J. 1983: Quantitative low-level acoustic sounding and comparison with direct measurements. *Boundary Layer Meteorol.* **27**, 1-26.
- Clifford, S.F. 1972, Propagation and scattering in a random media, *Remote Sensing of the Troposphere*, American Meteorological Society, Boston, 11-1–16-24.
- Coulter, R.L., 1990, A case study of turbulence in the stable nocturnal boundary layer, *Bound.-Layer Meteorol.* **52**, 75–91.
- Coulter, R.L., and Martin, T.J. 1986, Results from a high power, high frequency sodar, *Atmos. Res.* **20**, 257–270.
- Doran, J.C., Berkowitz, C.M., Coulter, R.L., Shaw, W.J., and Spicer, C.W. 2003, The 2001 Phoenix Sunrise experiment: Vertical mixing and chemistry during the morning transition in Phoenix, *Atmos. Environ.* **37**, 2365–2377.
- Kaimal, J. C. 1973: Turbulent spectra, length scales and structure parameters in the stable surface layer. *Boundary Layer Meteorol.* **4**, 289–309.
- Kristensen, L. 1978, *On Sodar Techniques*, Riso Report 381, Riso National Laboratory.

Mahrt, L., and Vickers, D. 2002, Contrasting vertical structures of nocturnal boundary layers, *Bound.-Layer Meteorol.* **105**, 351–363.

Thomson, D.W., Coulter, R.L., and Warhaft, Z. 1978, Simultaneous measurements of turbulence in the lower atmosphere using sodar and aircraft, *J. Appl. Meteorol.* **17**, 723–734.

Weill, A., Mazaudier, C., Leca, F., and Masmoudi, M. 1988, Doppler sodar and fluxes measurement, *Proc. 4th ISARS 1988*, Canberra, Australia, **30**, 1–6.